J. Indian Chem. Soc.,
Vol. 96, April 2019, pp. 455-460

Magnesium incorporated graphitic carbon nitride for effective removal of fluoride ions

Dimitra Das[a], Kalyan Kumar Chattopadhyay[b] and Somnath Mukherjee[c]*

[a]School of Materials Science and Nanotechnology, [b]Department of Physics, [c]Department of Civil Engineering,

Jadavpur University, Kolkata-700 032, India

E-mail: mukherjeesomnath19@gmail.com

Manuscript received online 01 February 2019, accepted 25 March 2019

In the present investigation, magnesium (Mg) doped graphitic carbon nitride (GCN) synthesized in nanotechnology laboratory has been used as a nano-adsorbent material for effective removal of fluoride (F^-) ions from water. The material has been characterized by different techniques like XRD, FTIR, and FESEM to get a detailed insight into their properties. The batch adsorption experiments have been performed by varying different influencing parameters viz. adsorbent amount, initial fluoride concentration and pH. The experimental data revealed that the adsorption capacity of fluoride by Mg doped GCN depends on the above parameters. The thermodynamic parameters, kinetic reaction orders and isotherm plots are also fitted in accordance with the conventional models based on experimental findings.

Keywords: Magnesium doping, graphitic carbon nitride, fluoride, isotherm modelling, adsorption kinetics.

Introduction

Fluoride in trace amount (0.6 mg/L, as per WHO) is one of the essential non-metals that have been considered favourable for bone and enamel developments for living mammals. However, fluoride ingestion in excessive amount can lead to severe detrimental effects like fluorosis[1]. In India, a large number of people of different states severely suffer from fluorosis whereas more than 62 million people remain exposed to it due to presence of excess fluoride level in ground water used for drinking[2,3]. Fluoride laden waste water also emanate from industries like glass manufacturing, rock phosphate production units etc. Several processes on fluoride removals are reported in the literatures but the most effective and common tool for fluoride attenuation process is adsorption as advocated by earlier researchers. Nalgonda technique[4] is one of the extensive adsorption methods used at large in India owing to its facile operative method. Activated charcoal, alumina, fish bone, charcoal, bio-chars, clay minerals etc. are used as adsorbent material for fluoride decontamination[5].

Recently nanomaterials are being applied for water and waste-water treatment as a smart and sustainable candidate for the above purpose. Graphitic carbon nitride is one such nanomaterial which possesses significant surface area and is easily synthesized from viable cheap precursor like urea in a large scale. The large surface helps in better adsorption of metal/non-metal ions depending upon the surface charge. However, pure GCN has a negative surface charge owing to the edge terminated nitrogen lone pairs that limits adsorption of fluoride ions. To overcome this restriction, GCN has been doped with magnesium which leads to the generation of a positive surface charge on the GCN layers thereby improving the surface adsorption properties. Mg is easily available, economic and environment friendly as compared to other available transition metals. The utilization of Mg doped GCN as a nano-adsorbent for fluoride removal from water environment is perhaps a new application of adsorption process.

Experimental

Urea (CH_4N_2O) and Magnesium chloride hexahydrate ($MgCl_2.6H_2O$) with 99.99% purity were used for synthesis purposes. In the synthesis procedure, requisite amount of $MgCl_2.6H_2O$ was intimately mixed with 10 g of urea in a mortar-pestle followed by drying the mixed product in an oven at 100ºC for 24 h. The dried product was then put in a well-covered crucible made of alumina accompanied with a lid in order to check any probable gas loss. The mixture was thermally treated in a muffle furnace at 550ºC for 4 h at 5ºC/min ramp. After allowing an ambient cooling in room temperature, a pale yellow to brownish yellow coloured powder samples were obtained. The products were named as X-MGCN (where X = 5 and 20 wt% of Mg doping). Pure graphitic carbon nitride was produced by directly heating urea at 550ºC for 4 h in a box furnace at the same rate of heating. The synthesis procedure is shown in Fig. 1.

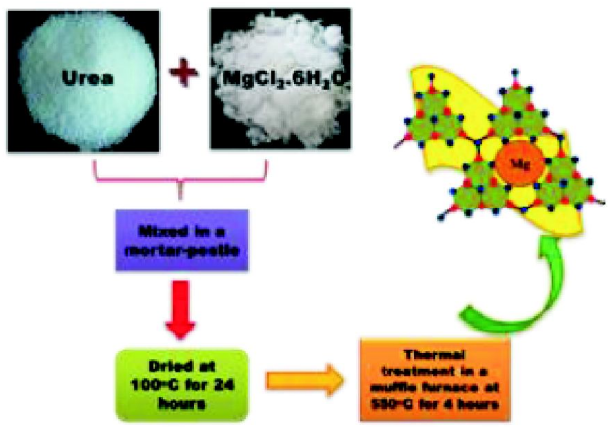

Fig. 1. Schematic representation of the synthesis procedure of Mg-GCN.

Several characterization techniques were subsequently performed for detailed analysis of the as prepared samples. X-Ray diffraction (XRD) studies were performed using Bruker D8 advanced diffractometer (1.2 kW, Cu Kα source λ = 1.5405 Å) whereas Fourier transform infrared (FTIR) spectroscopic studies were carried out by employing Shimadzu FTIR-8400S. Field emission scanning electron microscopic study (FESEM) was carried out using JEOL 6340F FEG-SEM.

Batch adsorption studies were conducted in a reciprocating type shaker device at a stirring speed of 150 rpm. 50 ml of spiked sample containing 6.1 mg/L fluoride was taken in a 100 ml polythene vial, with an adsorbent dose of 2 g/L. The mixture was thoroughly stirred in ambient condition for a period of 6 h. Samples were withdrawn at every 30 min interval up to a period of 6 h and residual concentration was analysed for fluoride (F^-) concentration. The F^- was analytically determined in ion selective meter (ISE) with F^- probe. Amount of adsorbent dose (0.5–10 g/L) were considered to examine the effects of sorbent mass on F^- removal. Batch adsorption studies were performed in the same manner to examine the effect of dosage. The equilibration dosage was considered to be 4 g/L. The effect of pH on F^- removal was conducted by different buffered pH solutions, viz. 2, 4, 6, 8, 10 and 12 with 6.1 mg/L of initial F^- concentration and equilibration adsorbent dosage of 4 g/L for an equilibration time of 180 min. The effect of initial F^- concentration was carried out with different initial F^- concentrations (2–10) mg/L.

Results and discussion

The XRD analysis (as shown in Fig. 2) was carried out to understand the phase formation of the as synthesized samples. The pure GCN sample shows the presence of two prominent peaks situated at 2θ = 13.1º and 27.4º corresponding to (100) and (002) diffraction planes respectively (JCPDS no. 87-1526)[6]. The sharp peak at 27.4º corresponds to the graphitic phase whereas the smaller hump at 13.1º corresponds to the melon units which act as the main building blocks of GCN. The 5 MGCN sample shows the characteristic (002) peak but there is absence of the peak corresponding to the (100) plane since introduction of Mg into GCN matrix occurs in between the melon units. It has been noted that the 20 MGCN sample exhibits a number of peaks along with the characteristic peak of GCN, all of which correspond to the different phases of Mg. The presence of $Mg(CO_3)_4.Mg(OH)_2.5H_2O$, $Mg(OH)_2$, $MgCO_3$ and MgO related phases are evident from Fig. 2.

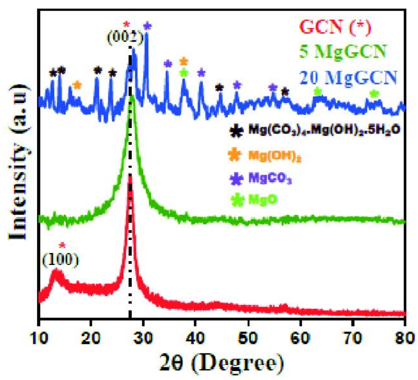

Fig. 2. XRD plots of GCN, 5 MGCN and 20 MGCN.

The FTIR spectra measured in transmittance mode with respect to wavenumber for all the samples are shown in Fig. 3. For pure GCN, the widely distributed hump centred around 3199 cm^{-1} occurs due to existence of residual amine groups resulting from incomplete polymerization during synthesis. The other prominent group of peaks distributed around 1200 cm^{-1} and 1650 cm^{-1} can be attributed to the stretching modes

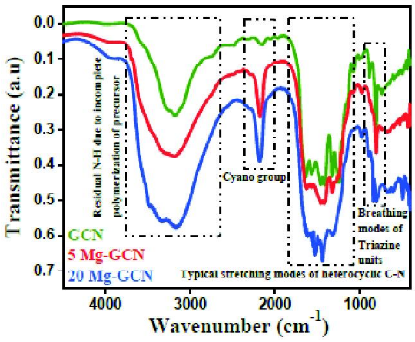

Fig. 3. FTIR spectra of GCN, 5 MGCN and 20 MGCN.

of vibrations of heterocyclic C-N bonds, the peak at 2170 cm^{-1} occurs due to cyano groups and finally the peak at 810 cm^{-1} are the main characteristic peak of GCN occurring due to breathing modes of vibrations of triazine units[7]. The 5 MGCN and 20 MGCN samples show all the characteristic peaks of GCN which indicates the impregnation of Mg or Mg related groups into the GCN matrix without altering the structural framework of host GCN. The 20 MGCN sample shows a broader hump near 3179 cm^{-1} which is probably due to the presence of hydroxyl groups associated with Mg. The peak corresponding to the cyano groups (at 2170 cm^{-1}) becomes more intense for 20 Mg-GCN which reveals the interaction of Mg with -C≡N bond.

The morphology of the samples is evident from the FESEM images as shown in Fig. 4(a and b). Fig. 4(a) shows the two dimensional sheet like morphology of the pure GCN sample. However, it is evident from Fig. 4(b) that there is co-existence of both sheet like GCN and rod like Mg groups in 20 MGCN sample which in turn proves the formation of the nanocomposite.

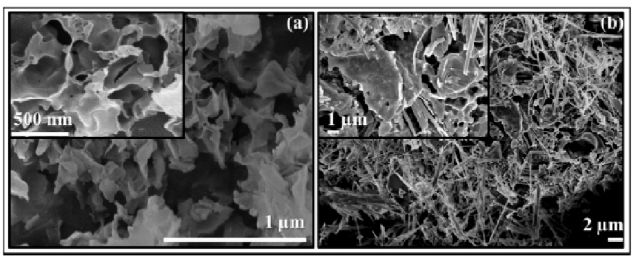

Fig. 4. FESEM images of (a) GCN and (b) 20 MGCN.

The amount of F$^-$ adsorbed per unit mass (q_e) is calculated as[8]

$$q_e = (C_i - C_e)V/m \quad (1)$$

where C_i and C_e are the initial and equilibrium concentration of F$^-$ ions (mg/L), m is the mass of the adsorbent (g) and V is the volume of the solution (mL). The percentage of fluoride removal is calculated as

$$\%R = [(C_i - C_e)/C_i]\times 100 \quad (2)$$

It is observed from Fig. 5 that pure GCN at a concentration of 2 g/L shows inferior F$^-$ removal capability with initial F$^-$ concentration of 5 mg/L even after 180 min of contact time. However, with incorporation of Mg into GCN matrix, the F$^-$ removal capability is increased and the highest percentage of Mg impregnated GCN nanomaterial exhibited significantly enhanced removal efficiency of about 78% within the same contact time.

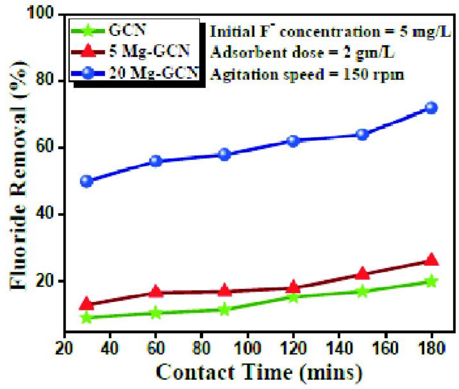

Fig. 5. Fluoride removal efficiency by GCN, 5 MGCN and 20 MGCN.

The effect of contact time on the removal efficiency with an initial F$^-$ concentration of 6.1 mg/L and an adsorbent dosage of 2 g/L is exhibited in Fig. 6. It is observed that 78% removal efficiency has been achieved within 180 min of con-

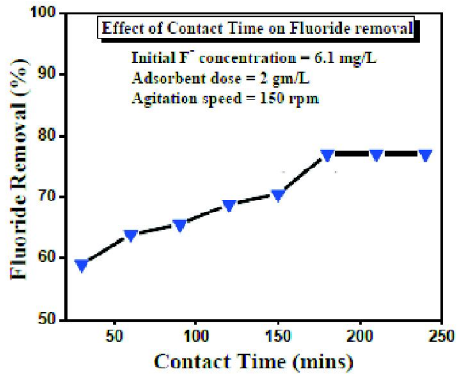

Fig. 6. Effect of contact time on F$^-$ removal efficiency by 20 MGCN.

tact time after which the F^- removal capacity was found to be marginal. Hence the equilibration time is considered to be 180 min. With increase in the contact time, the net surface coverage of the 20 MGCN adsorbent becomes high, i.e. the number of active sites on the surface of the adsorbent becomes depleted for which further adsorption after the equilibration time is not attainable. The effect of dosage of the 20 MGCN adsorbent on F^- removal efficiency is shown in Fig. 7. The adsorbent was added in varying amounts from 0.5 to 10 g/L and the maximum removal efficiency of about 87% was obtained for 4 g/L of adsorbent dose with an initial F^- concentration of 6.1 mg/L and contact time of 180 min. It is noted that beyond 4 g/L of dosage, no further F^- removal took place. At a lower concentration of the adsorbent, the

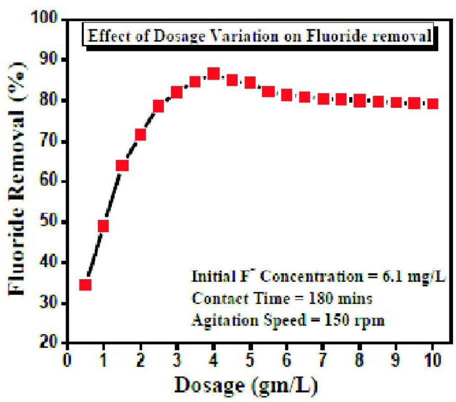

Fig. 7. Effect of varying adsorbent dosage on F^- removal efficiency by 20 MGCN.

number of surface active sites is much higher. With the increase in the 20 MGCN dosage, aggregation of the adsorbent particles occurs which hinders the removal efficiency to a great extent. The migration of F^- due to higher Zeta potential at lower dose was prominent.The effect of pH on the F^- removal efficiency was subsequently studied by varying the pH of the solution from 2 to 12 with an initial F^- concentration of 6.1 mg/L, adsorbent dosage of 4 g/L and at a contact time of 180 min. It has been observed from Fig. 8 that the maximum removal efficiency of about 98% was obtained at a pH value of 6 and the efficiency decreased significantly at higher pH values. At basic pH values, the surface of the adsorbent becomes negatively charged. Hence repulsion occurs between the negatively charged F^- ions and the adsor-

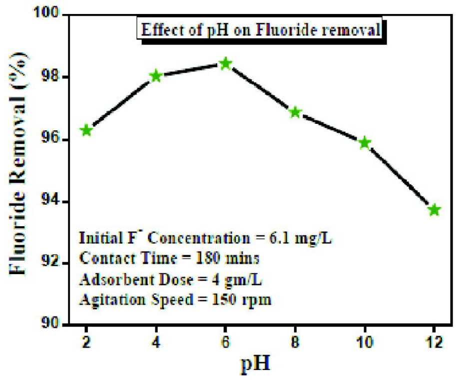

Fig. 8. Effect of pH on F^- removal efficiency by 20 MGCN.

bent surface which decreases the adsorption capability of the adsorbent. This results in the decreased removal efficiency at higher pH. Finally the effect of initial F^- concentration on the removal efficiency is analysed to see the maximum initial concentration which can be imposed on the nanocomposite material for effective removal. The corresponding graph is shown in Fig. 9. It is observed that in correspondence to an adsorbent dosage of 4 g/L and contact time of 180 min, the fluoride removal efficiency increases with the increase in the initial fluoride concentration and the maximum removal efficiency of 98% was achieved at F^- concentration of 10 mg/L. The efficiency decreased considerably after further increase in the F^- concentration.

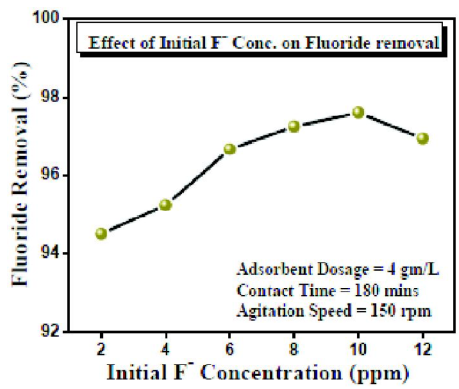

Fig. 9. Effect of initial F^- concentration on F^- removal efficiency by 20 MGCN.

The isotherm studies were performed to understand the adsorption mechanism and its thermodynamic aspects along with the interaction of the adsorbate on the adsorbent. The isotherm plots were fitted by two conventional Langmuir and Freundlich isotherm models. The Langmuir isotherm is represented by the equation

$$C_e/q_e = (1/K_L q_e) + (C_e/q_{max}) \quad (3)$$

where K_L is the Langmuir constant (mg^{-1}) and q_{max} determines the maximum adsorption capacity (mg/g). The Langmuir isotherm as shown in Fig. 10 is basically the linear plot of specific adsorption (C_e/q_e) against the equilibrium concentration (C_e)[9].

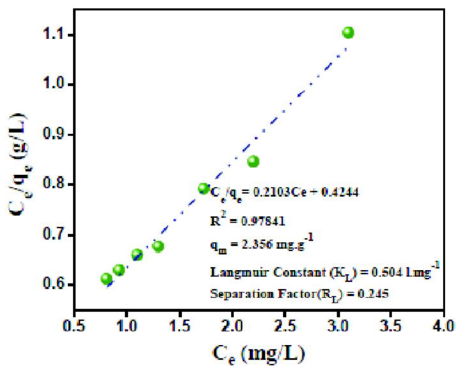

Fig. 10. Langmuir isotherm plot for adsorption of F$^-$ ions by 20 MGCN.

The maximum adsorption capacity as determined from the Langmuir isotherm plot is 2.356 mg/g. The separation factor (R_L) is one of the necessary isotherm parameters used to define the affinity between the adsorbate and the adsorbent. This dimensionless equilibrium parameter is calculated from the equation[9],

$$R_L = 1/(1+ K_L C_i) \quad (4)$$

The value of the R_L provides significant information regarding the nature of the adsorption. If the value lies between 0 and 1, it indicates favourable adsorption. The value of R_L as obtained in this case is 0.245 thus establishing the favourable nature of the adsorption.

The Freundlich isotherm model is described by the equation[9],

$$\ln (q_e) = \ln K_F + (1/n) \ln (C_e) \quad (5)$$

K_F is the Freundlich constant which measures the adsorption capacity and '*n*' is the adsorption intensity. These constants K_F and *n* are elucidated from the intercept and the slope of the linear plot of ln (q_e) vs ln (C_e) respectively. The adsorption intensity is estimated from the plot as 1.4646, and since this value is greater than 1, hence it indicates favourable adsorption phenomenon. The nature of the adsorption is physical in nature. The plot is shown in Fig. 11.

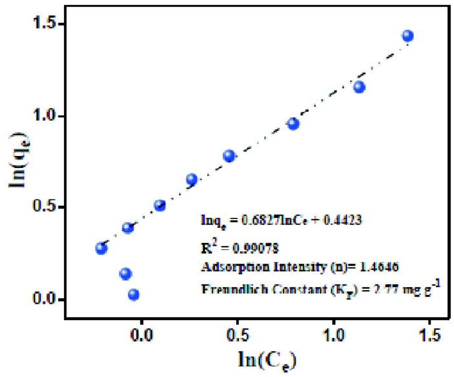

Fig. 11. Freundlich isotherm plot for adsorption of F$^-$ ions by 20 MGCN.

Since the adsorption isotherm is well fitted (R^2 = 0.99) by the Freundlich model, that indicates the multilayer adsorption nature of F$^-$ ions on 20 MGCN. The reaction follows the pseudo-first order kinetics model which follows the equation

$$\ln (q_e - q_t) = \ln (q_e) - k_1 t \quad (6)$$

where q_e and q_t are the amount of F$^-$ ions adsorbed per mass of adsorbent (mg/g) at equilibrium and at any time '*t*' respectively. ln (q_e) is obtained as the slope and k_1 as the intercept from the linear plot of ln ($q_e - q_t$) vs time. k_1 is the pseudo-first order rate constant. The corresponding plot is shown in Fig. 12. The well fitted plot of the pseudo-first order model indicates the occurrence of physisorption of F$^-$ ions on 20 MGCN.

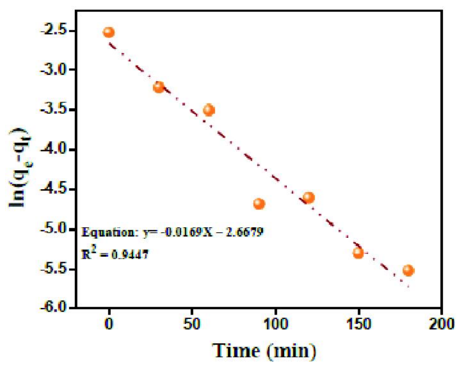

Fig. 12. Pseudo-first order kinetics model for F$^-$ adsorption.

Fig. 13 depicts the plausible mechanism of F^- adsorption on 20 MGCN nanocomposite. GCN in its pure form was unable to adsorb F^- ions on its surface due to the absence of any surface functional groups and active sites. Moreover the negative surface charge arising from the lone pairs of edge terminated nitrogen atoms hindered the interaction with negatively charged F^- ions. Furthermore, MgO and related groups get lesser opportunity from agglomeration tendency[10]. Hence they need a stable matrix for their performance. In the present work, GCN provides a stable matrix for the incorporation and attachment of Mg related groups. Magnesium has high affinity for F^- ions which results in the significant adsorption of F^- ions on 20 MGCN adsorbent. Moreover impregnation of Mg related groups renders positive surface charge on GCN matrix which in turn enhances the adsorption property.

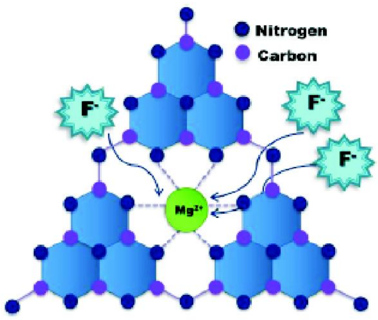

Fig. 13. Schematic representation of F^- adsorption on 20 MGCN adsorbent**.**

Conclusions

In conclusion, the present work reports the successful development of the 20 MGCN nanomaterial and its effective utilization in the removal of fluoride ions from water environment. The series of batch studies performed revealed the effect of various parameters on the adsorption property of 20 MGCN. The experimental results are well fitted in adsorption isotherms and also found to follow pseudo-first order kinetics model. It is proposed to investigate further with the reported material for treating different pollutants from water environment both in laboratory and in real life situation.

Acknowledgements

The authors thank the UGC, India for UPE II scheme. DD thanks DST [Reg. No. of DD-IF170684], India for providing the DST-Inspire fellowship.

References

1. B. Nagappa and G. T. Chandrappa, *Microporous Mesoporous Mater.*, 2007, **106**, 212.
2. N. Minju, K. Venkat Swaroop, K. Haribabu, V. Sivasubramanian and P. Senthil Kumar, *Desalin. Water Treat.*, 2015, **53**, 2905.
3. D. Mohapatra, D. Mishra, S. P. Mishra, G. R. Chaudhury and R. P. Das, *J. Colloid Interface Sci.*, 2004, **275**, 355.
4. R. L. Droste and R. L. Gehr, "Theory and practice of water and wastewater treatment", John Wiley & Sons, 2018.
5. A. M. Raichur and M. J. Basu, *Sep. Purif. Technol.*, 2001, **24**, 121.
6. F. Fina, S. K. Callear, G. M. Carins and J. T. Irvine, *Chem. Mater.*, 2015, **27**, 2612.
7. D. Das, D. Banerjee, M. Mondal, A. Shett, B. Das, N. S. Das, U. K. Ghorai and K. K. Chattopadhyay, *Mater. Res. Bull.*, 2018, **101**, 291.
8. M. B. Desta, *J. Thermodynamics*, 2013.
9. K. D. Kowanga, E. Gatebe, G. O. Mauti and E. M. Mauti, *The J. Phytopharmacology*, 2016, **5**, 71.
10. L. L. Ling, W. J. Liu, S. Zhang and H. Jiang, *Environ. Sci. Technol.*, 2017, **51**, 10081.

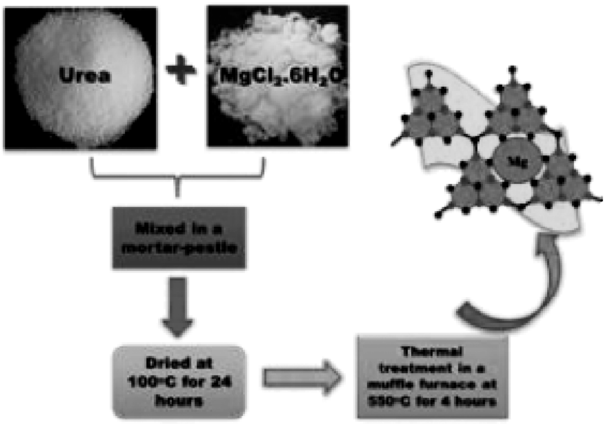
Urea
MgCl2.6H2O
Mg
Mixed in a mortar-pestle
Dried at 100°C for 24 hours
Thermal treatment in a muffle furnace at 550°C for 4 hours

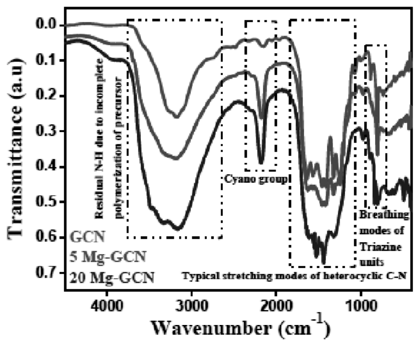
Transmittance (a.u)
Wavenumber (cm-1)
Residual N-H due to incomplete polymerization of precursor
Cyano group
Breathing modes of Triazine units
Typical stretching modes of heterocyclic C-N
GCN
5 Mg-GCN
20 Mg-GCN

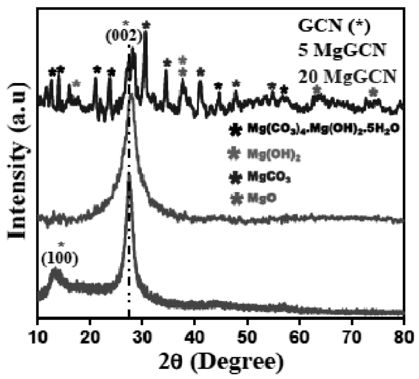
Intensity (a.u)
2θ (Degree)
GCN (*)
5 MgGCN
20 MgGCN
(002)
(100)
Mg(CO3)4.Mg(OH)2.5H2O
Mg(OH)2
MgCO3
MgO